

## Exact simulations of quantum rings and characterization of hexanuclear manganese and dodecanuclear nickel cyclic complexes

This article has been downloaded from IOPscience. Please scroll down to see the full text article.

2001 J. Phys.: Condens. Matter 13 2017

(<http://iopscience.iop.org/0953-8984/13/9/325>)

View [the table of contents for this issue](#), or go to the [journal homepage](#) for more

Download details:

IP Address: 171.66.16.226

The article was downloaded on 16/05/2010 at 08:46

Please note that [terms and conditions apply](#).

# Exact simulations of quantum rings and characterization of hexanuclear manganese and dodecanuclear nickel cyclic complexes

A Caramico D'Auria<sup>1</sup>, U Esposito<sup>1</sup>, F Esposito<sup>1</sup>, G Kamieniarz<sup>2</sup> and R Matysiak<sup>3</sup>

<sup>1</sup> Dipartimento di Scienze Fisiche, Università di Napoli 'Federico II', Piazzale Tecchio, 80125 Napoli and INFN Unità di Napoli, Italy

<sup>2</sup> Computational Physics Division, Institute of Physics, A Mickiewicz University, ulica Umultowska 85, 61-614 Poznań, Poland

<sup>3</sup> Institute of Technology, Pedagogical University in Zielona Góra, Poland

E-mail: filesp@na.infn.it (F Esposito) and gjk@amu.edu.pl (G Kamieniarz)

Received 25 April 2000, in final form 7 December 2000

## Abstract

A numerical transfer-matrix approach and diagonalization technique exploiting the point-group symmetry are worked out in the framework of quantum statistical mechanics and group theory as exact simulation tools for application to thermodynamical properties of finite rings. They are applied to the isotropic spin models of the high-nuclearity cyclic clusters  $[\text{Mn}(\text{hfac})_2\text{NITPh}]_6$  and  $\text{Ni}_{12}(\text{O}_2\text{CMe})_{12}(\text{chp})_{12}(\text{H}_2\text{O})_6(\text{THF})_6$ . The microscopic parameters of both molecules ( $J/k_B = 350 \pm 10$  K and  $J/k_B = 8.5 \pm 0.5$  K, respectively, with  $g = 2.23 \pm 0.01$ ) are then obtained from a fit of the theoretical susceptibility curves to the experimental results.

Polynuclear clusters provide magnetic materials with a scale intermediate between that of isolated dimers or trimers and that of bulk magnetic materials [1–5]. These magnetic materials exhibit features on a mesoscopic scale, so they may show quantum effects coexisting with classical behaviour and various new properties. Also, large metal-ion clusters are present in biological systems (e.g. ferritin [1]) and the modelling of their properties is under way. In addition, large assemblies of spins are interesting as real objects on which to test theoretical models with a finite number of spins.

Characterization of polynuclear magnetic aggregates remains a challenging task [6, 7]. They have well defined molecular weights and crystal structures [1], allowing quantitative comparison of experimental results with theory. Unlike other assemblies of small magnetic particles with size and/or shape distributions, a typical sample of a molecular magnetic compound is composed of nominally identical non-interacting magnets with a unique set of chemically determined parameters. They are complex organometallic systems, too difficult to approach by the *ab initio* methods applicable to simple metal clusters [8–12].

The usual way to characterize molecular magnets is by modelling them in terms of spin Hamiltonians [1]. Polynuclear magnetic clusters are formed by magnetic centres with different values  $S$  of the spin and different geometrical structures. The main difficulty in the theoretical model calculations is the exponential increase in computational complexity with the number of spins  $N$ . With increasing value of the spin  $S$  and the symmetry decreasing due to more complicated geometrical structure or due to alternation of the value of  $S$  or variation of the value of the interactions, spin model calculations are limited to small systems. Quantitative interpretations are available only in a few fortuitous cases.

The aim of this paper is to present exact simulation techniques for characterizing quantitatively the thermodynamical properties of the high-nuclearity rings  $[\text{Mn}(\text{hfac})_2\text{NITPh}]_6$  and  $\text{Ni}_{12}(\text{O}_2\text{CMe}_{12}(\text{chp})_{12}(\text{H}_2\text{O})_6(\text{THF})_6)$  and to estimate their model parameters. The complexes are referred to as the supramolecular clusters  $\text{Mn}_6$  and  $\text{Ni}_{12}$ , respectively. They have already undergone a qualitative analysis [2, 4]. Their common feature is the unusual spin  $S = 12$  ground state, a state showing one of the highest spin multiplicities observed for a molecular species [1, 2, 4].

As to the geometrical structure, the  $\text{Mn}_6$  molecule contains twelve paramagnetic centres [1, 4]—namely six manganese (II)  $S = 5/2$  ions and six organic radicals, NITPh, each with an unpaired  $S = 1/2$  electron. Qualitative theoretical consideration related to the zero-field susceptibility measurements led to the conclusion that the magnetic properties can be explained by a strong antiferromagnetic coupling  $|J| > 250$  K [1, 4] between the two types of spin.

The  $\text{Ni}_{12}$  cluster [2] is a dodecanuclear metallocyclic complex, which contains a ring of twelve  $S = 1$  Ni centres. The nickel ions are bridged by intersecting  $\text{Ni}_2\text{O}_2$  rings and the clusters are not subject to significant intermolecular interactions. The measurements of the effective magnetic moment for  $T > 4.2$  K and subsequent approximate analysis have shown that the magnetic properties of  $\text{Ni}_{12}$  can be explained by a ferromagnetic coupling inside the ring, estimated as  $J = 13.5$  K [2]. The crystal structure of  $\text{Ni}_{12}$  resembles that of decanuclear  $[\text{Fe}(\text{OMe})_2(\text{O}_2\text{CCH}_2\text{Cl})_{10}]_{10}$ , known as the ferric wheel [3], displaying interesting quantum effects in bulk magnetic measurements.

The form of the spin Hamiltonian modelling the system is mainly determined by the spin of the magnetic carriers and the topology of the molecular structure. It depends also on the quality of the sample, the temperature and the type of measurement. In the case of susceptibility measurements performed for the powder sample, it is difficult to fit the data in order to estimate the anisotropy parameters. For the high-temperature data it is even impossible. The usual procedure is to establish the magnetic exchange coupling from the bulk magnetic measurements and then to determine the anisotropy parameters by means of more refined experiments probing the energy structure. To characterize the finite-temperature properties of  $\text{Mn}_6$  and  $\text{Ni}_{12}$ , we consider the rings in the framework of the isotropic spin model Hamiltonian

$$\mathcal{H} = - \sum_{i=1}^N (JS_i S_{i+1} + g\mu_B B S_i^z) \quad (1)$$

where  $J$  denotes the nearest-neighbour interaction constant (positive for ferromagnetic coupling),  $B$  is the external magnetic field applied along the  $z$ -direction,  $g$  is the corresponding gyromagnetic ratio and  $N$  stands for the number of sites in the ring ( $N + 1 \rightarrow 1$ ). The spin value  $S_i$  may be uniform ( $S = 1$  for the  $\text{Ni}_{12}$  molecule) or non-uniform (for the  $\text{Mn}_6$  cluster). In the latter case,  $S = \frac{5}{2}$  for odd sites  $i$  and  $S = \frac{1}{2}$  for even sites  $i$ .

Using symmetry arguments, the quantum Hamiltonian (1) has been repeatedly diagonalized numerically for uniform spin  $S = 1/2$  [13, 14] and more recently for uniform spin  $S = 1$  and non-uniform interactions [15], or for non-uniform  $S$  and uniform interactions [6].

The most successful approach which has been developed for the polynuclear clusters is based on the irreducible tensor operator (ITO) method [6].

In this paper we present two different exact simulation schemes yielding the thermodynamic properties of model (1): the quantum transfer-matrix (QTM) method and the diagonalization method exploiting the point-group symmetry. The QTM is adapted for use with model (1) with a non-uniform spin variable. Although the single-ion anisotropy terms, both longitudinal and transverse, and the non-uniform interactions could also be included, the experimental data available to us do not justify this extra effort. As to our diagonalization method, its primary advantage is that it implements the idea of applying the corresponding shift operator to take into account the translational (or rotational) symmetry. This idea and the group-theory arguments enable an effective coding to be achieved and provide a reduction of the corresponding invariant subspaces to sizes smaller than that within the ITO method. Finally, the numerical diagonalization of larger systems (1) can be accomplished here.

First we briefly describe the QTM simulation method for a finite ring with two alternating spin values  $S_i$  ( $i = 1, 2$ ). Previously, a similar method was applied both to the macroscopic  $S = 1$  Haldane-gap systems and to the  $S = 1$  molecule-based chains with both uniform and non-uniform couplings as well as single-ion anisotropy [16, 17]. It is not subject to any statistical or systematic errors and, as far as the macroscopic chains are concerned, the corresponding free energy can be directly evaluated from the largest eigenvalue of the transfer matrix.

Within the QTM method we may calculate some classical approximants of the thermodynamic functions and then recover the quantum regime, by taking the appropriate limit. The series of classical approximants of the quantum thermal values can be found using the general Suzuki–Trotter formula [16, 18]. Then the partition function can be calculated from the expression

$$\mathcal{Z} = \lim_{m \rightarrow \infty} \mathcal{Z}_m = \lim_{m \rightarrow \infty} \text{Tr} \left[ \prod_{i=1}^N e^{-\beta \mathcal{H}_{i,i+1}/m} \right]^m \quad (2)$$

where the trace is taken over all of the configurations of the classical Ising variable  $S_{ij}$  (the eigenvalues of  $S_{ij}^z$ ) on a planar lattice of size  $N \times 2m$ ,  $m$  is an integer referred to as the Trotter index and  $\mathcal{H}_{i,i+1}$  stands for the corresponding spin-pair Hamiltonian. Periodic boundary conditions ( $N+1 \rightarrow 1$ ) are imposed to account for the cyclic character of the physical objects. The zero-field susceptibility is then evaluated from the second derivative of the free energy with respect to the field.

For the system with non-uniform spin values, the numerical implementation of (2) is based on two global transfer operators  $\mathcal{W}_i$  ( $i = 1, 2$ ) acting in the space  $\mathcal{H}^N$  which is a direct product of  $N$  single-spin spaces  $\mathcal{H}_i$ . The final expression is given by

$$\mathcal{Z}_m = \text{Tr}(\mathcal{W}_1 \mathcal{W}_2)^m \quad (3)$$

where

$$\mathcal{W}_i = (\mathcal{V}_i \mathcal{P}^+)^{N/2} \quad i = 1, 2.$$

$\mathcal{P}$  and  $\mathcal{V}_i$  ( $i = 1, 2$ ) stand for a unitary shift operator and a local transfer operator, respectively [18]. The explicit form of the operator  $\mathcal{V}_i$  depends on the choice of the spin operators in Hamiltonian (1) whereas that of  $\mathcal{P}$  is universal.

The QTM technique described here can be applied to model (1) with both uniform and non-uniform spin variables. In the case of a uniform spin variable  $S = 1$  and  $N = 12$  (appropriate for  $\text{Ni}_{12}$ ), the computational cost of our technique would be relatively low compared with that for  $\text{Mn}_6$ . We emphasize that, in contrast to the case for the macroscopic limit, in our

simulations the full trace in (3) has to be taken and we consider the index  $m$  large enough to get estimates of the partition function (2) up to at least four decimal places.

In our diagonalization technique, the translational symmetry of the Hamiltonian (1) is described in terms of the unitary shift operator  $\mathcal{P}$ , which commutes with  $\mathcal{H}$  and the  $z$ -component of the total spin  $S^z$ . The eigenvalues of  $\mathcal{P}$  are the  $N$ th-order roots of 1 and the corresponding eigenvectors are complex linear combinations of the basis vectors. To avoid complex numbers which increase the storage requirements, we have introduced the real operator  $\frac{1}{2}(\mathcal{P} + \mathcal{P}^\dagger)$ . The invariant subspaces of this operator have bigger dimensions but we can recover the reduction by a factor of  $N$ , by including in our analysis the reflection symmetry. This leaves all previously defined subspaces invariant and the associated operator  $\mathcal{R}$  has the eigenvalues  $+1$  and  $-1$ . As Hamiltonian (1) commutes with rotations (translations) and reflections, the whole matrix is factorized in blocks labelled by the following quantum numbers: the  $z$ -component of the total spin  $S_z = 0, \pm 1, \pm 2, \dots, \pm N$ ; the shift-symmetry eigenvalue  $k$  ( $0 \leq k \leq N/2$ ); the reflection eigenvalue  $R = \pm 1$ . The dimensions of blocks are determined by the computer algorithm and for  $S_z = 0$  are listed in table 1. In this way the largest invariant subspace has the dimension 6166 for  $N = 12$  and  $S = 1$ . The task of diagonalizing matrices of this size can be carried out by present-day computers and the whole spectrum of Hamiltonian (1) can be ‘exactly’ calculated. Afterwards, any thermodynamic function can be easily obtained at an arbitrary temperature, using the standard formulae without an extra computational cost. With the present technique, we have reached sizes of matrices as small as those for the group-theoretical combinatorial approach [19]. Moreover, we have determined the corresponding matrix elements allowing the subsequent diagonalization.

**Table 1.** Block dimensions of the  $S_z = 0$  Hamiltonian submatrices classified according to the shift index  $k$  and the reflection eigenvalue  $R$ .

| $k$ | $R$     | Dimension |
|-----|---------|-----------|
| 0   | +1      | 6166      |
| 6   | -1      | 6163      |
| 1   | $\pm 1$ | 6136      |
| 2   | $\pm 1$ | 6158      |
| 3   | $\pm 1$ | 6140      |
| 4   | $\pm 1$ | 6160      |
| 5   | $\pm 1$ | 6136      |

As to the numerical results, the QTM approach is applied here to calculate the susceptibility of the ring with alternating spins  $S_A = \frac{5}{2}$ ,  $S_B = \frac{1}{2}$ . For a finite  $N = 12$ , the full trace in (2) has to be taken into account and the size of the transfer matrix blows up to  $[(2S_A + 1)(2S_B + 1)]^{N/2} = 2985984$ . We have carefully checked the convergence of our results with respect to the length in the Trotter direction and we compared the final estimates with those available in table 4 of [6]. In order to reach the accuracy up to the fifth decimal place for  $2 \leq n = N/2 \leq 4$  spin pairs, we had to carry out  $200 \leq m \leq 900$  steps in the Trotter direction, depending on  $n$  and on temperature. For  $n = 5$  and accuracy up to the fourth decimal place, 50 steps were sufficient. To avoid using an excessive amount of supercomputer time, we have mainly carried out the simulations up to  $n = 5$  pairs.

To characterize  $[\text{Mn}(\text{hfac})_2\text{NITPh}]_6$ , which consists of six spin pairs, we have estimated the zero-field susceptibility from the extrapolations of the data for the values  $2 \leq n \leq 5$  (our preliminary results for  $\text{Mn}_6$  have been published elsewhere [20]). A rather good convergence in terms of  $n$ , sufficient for our purposes, has been obtained down to  $k_B T/J = 0.05$ . Due to the increasing quantum fluctuations, the uncertainty of our prediction at the lowest temperature

has increased to of the order of 5%. For that reason, to verify our results, we have undertaken QTM simulations of the system with the full number  $n = 6$  of spin pairs at  $k_B T/J = 0.05$ . The corresponding numerically ‘exact’ estimate (up to the fourth decimal place) of the zero-field susceptibility is plotted as the large full circle in figure 1, yielding an excellent confirmation of the approximate calculations.

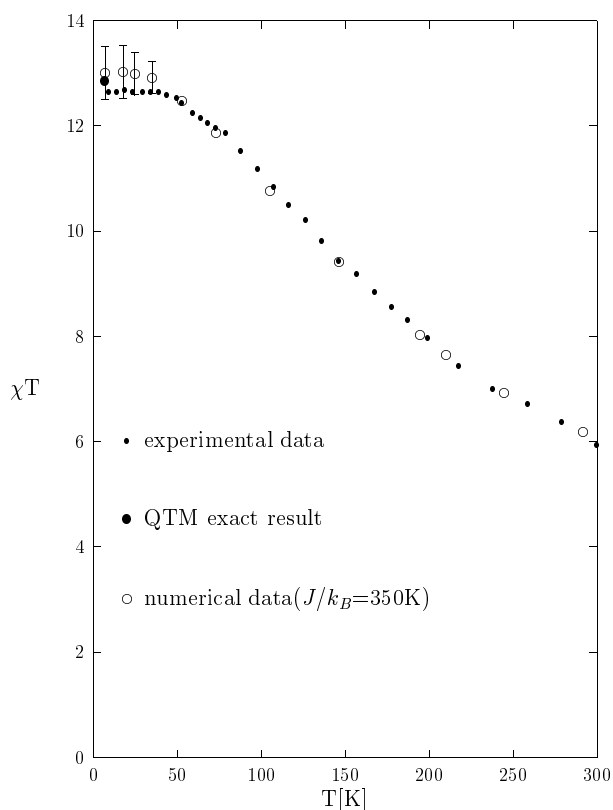


**Figure 1.** The temperature dependence of the product  $T\chi$  for  $\text{Mn}_6$  in molar units ( $\text{emu K mol}^{-1}$ ) divided by the number of pairs. The experimental data are given by the small full circles and the extrapolated QTM results by the open circles. The large full circle shows the numerically exact QTM estimate at  $k_B T/J = 0.05$ . The error bars are indicated where they exceed the size of the symbol.

In view of the negligible spin–orbit coupling, we have fixed  $g = 2$  and we have determined the isotropic coupling constant  $J/k_B = 350 \pm 10$  K from the best fit to experiment. This result is consistent with the existing qualitative estimates [1,4]. The temperature dependence of our predictions of  $T\chi$  for  $[\text{Mn}(\text{hfac})_2\text{NITPh}]_6$ , expressed for the monomeric formula [4], is displayed in figure 1. Numerical data plotted as open circles agree, within the error bars, with the susceptibility measurements (small full circles) of the real compound and with the exact value given by the large full circle.

The fitting procedure for  $\text{Ni}_{12}$  was performed in the framework of the isotropic model (1), neglecting the crystal-field effects [2, 21, 22]. In figure 2, the experimental product  $T\chi$  (shown as full circles) for the  $\text{Ni}_{12}$  complex is plotted as a function of temperature. The data are converted from those expressing the effective magnetic moment per formula unit [2]. The best fit is achieved for the parameters  $J/k_B = 8.5 \pm 0.5$  K,  $g = 2.23 \pm 0.01$ , consistent with

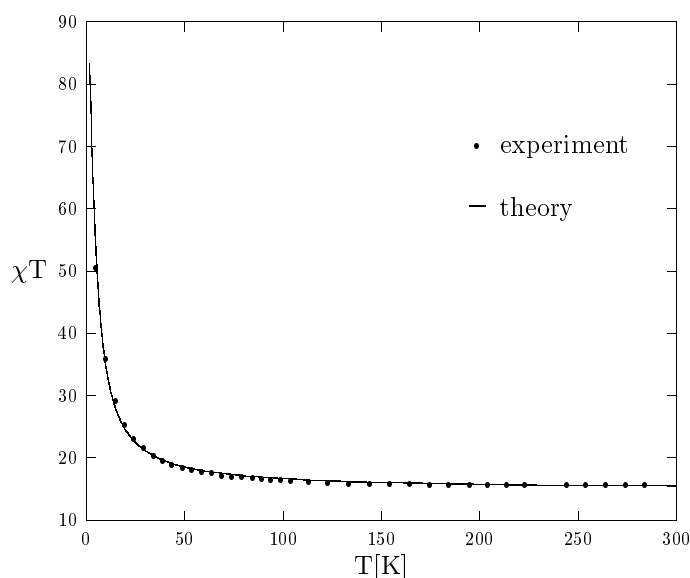


**Figure 2.** The temperature behaviour of  $T\chi$  for  $\text{Ni}_{12}$  in molar units ( $\text{emu K mol}^{-1}$ ). The experimental data are plotted as full circles and our numerical estimates are shown by the full line.

those previously reported [2]. The theoretical curve is shown as the full line and it interpolates very well between the measured values.

For the  $\text{Ni}_{12}$  aggregate the isotropic model (1) should be considered as a first approximation. However, the measurements of the susceptibility were performed on the powder sample at relatively high temperatures ( $k_B T/J \geq 0.5$ ), so the explicit anisotropy effects are absent from the experimental results and an attempt to fit the data with more than one parameter would be rather unrealistic. Our calculations yield strong evidence that the system in question can be described by the ferromagnetic model (1) with a given coupling constant.

In conclusion, we have worked out two effective numerical approaches suitable for characterizing the finite-temperature magnetic properties of high-nuclearity cyclic spin clusters with large and alternating spins and we have also carried out simulations for the title compounds.

The QTM technique can provide numerically exact results if the dimensionality of the multispin space allows the performing of the trace operation in the definition of the partition function (3). This is the case both for  $\text{Mn}_6$  and for  $\text{Ni}_{12}$  clusters. If it was not feasible, the technique could be still used after a change of the direction of transfer and subsequent extrapolations.

Within the QTM method, a quantitative interpretation of the susceptibility measurements for  $\text{Mn}_6$  has been accomplished here. We could follow this strategy for the  $\text{Ni}_{12}$  system, but our algebraic group-theoretical approach led us to reduce the dimensionality of the total spin-component subspaces of the isotropic model (1) at least down to 6166. At this level of complexity, diagonalization has proved a very efficient way of achieving quantitative characterization of the thermodynamic properties of the  $\text{Ni}_{12}$  complex, in agreement with experiment.

We have also found the energy spectrum of  $\text{Ni}_{12}$ . The ground state corresponds to  $S = 12$  and there is an excited state that is 46-fold degenerate at the energy level  $E/k_B = 0.2680$ ,  $J/k_B = 2.278$  K. At the moment we cannot specify the excited state by the total spin  $S$ , but this could be accomplished easily. Moreover, if any EPR or neutron

scattering experiment was performed for Ni<sub>12</sub>, our diagonalization technique could be adapted to take into account the anisotropy effects.

We would like to point out that the QTM approach is particularly effective and can be exploited for other polynuclear clusters. After some modifications it will also be suitable for application to systems with crystal-field anisotropy and alternating bonds, so the isotropic limit for Ni<sub>12</sub> could be relaxed as far as the thermodynamic properties are concerned.

### Acknowledgments

We would like to thank Professors Dante Gatteschi, Cristiano Benelli and Roberta Sessoli for very helpful discussions. This work was supported in part by the Committee for Scientific Research under the KBN grant No 8 T11F 027 16. The numerical calculations were mainly carried out on the platforms of the Supercomputing and Networking Centre in Poznań. One of us (GK) would like to acknowledge the warm hospitality of and financial support from the University of Naples 'Federico II' where this work was completed.

### References

- [1] Gatteschi D, Caneschi A, Pardi L and Sessoli R 1994 *Science* **265** 1054
- [2] Blake A J, Grant C M, Parsons S, Rawson J M and Winpenny R E P 1994 *J. Chem. Soc., Chem. Commun.* 2363
- [3] Taft K L, Delfs C D, Papaefthymiou G C, Foner S, Gatteschi D and Lippard S 1994 *J. Am. Chem. Soc.* **116** 823
- [4] Caneschi A, Gatteschi D, Laugier J, Rey P, Sessoli R and Zanchini C 1988 *J. Am. Chem. Soc.* **110** 2795
- [5] Müller A, Shah S Q N, Bögge H and Schmidtman M 1999 *Nature* **397** 48
- [6] Gatteschi D and Pardi L 1993 *Gazz. Chim. Ital.* **123** 231
- [7] Lascialfari A, Gatteschi D, Borsa F and Cornia A 1997 *Phys. Rev. B* **55** 14 341
- [8] Viitala E, Häkkinen H, Manninen M and Timonen J 2000 *Phys. Rev. B* **61** 8851
- [9] Reuse F A, Khana S N and Bernel S 1995 *Phys. Rev. B* **650** 11 650
- [10] Cheng H and Wang L-S 1996 *Phys. Rev. Lett.* **77** 51
- [11] Pappas D P, Popov A P, Anisimov A N, Reddy B V and Khana S N 1996 *Phys. Rev. Lett.* **76** 4332
- [12] Piveteau B, Desjonquères M-C, Oleś A M and Spanjaard D 1996 *Phys. Rev. B* **53** 9251
- [13] Bonner J C and Fisher M E 1964 *Phys. Rev.* **135** A640
- [14] Fabricius K, Löw U, Mütter K H and Ueberholtz P 1991 *Phys. Rev. B* **44** 7476
- [15] Borrás-Almenar J J, Coronado E, Curely J and Georges R 1995 *Inorg. Chem.* **34** 2699
- [16] Kamieniarz G, Matysiak R, Caramico D'Auria A, Esposito F and Esposito U 1997 *Phys. Rev. B* **56** 645
- [17] Caramico D'Auria A, Esposito F, Esposito U, Gatteschi D, Kamieniarz G and Wałcerz S 1998 *J. Chem. Phys.* **109** 1613
- [18] Delica T and Leshke H 1990 *Physica A* **168** 736
- [19] Kamieniarz G, Matysiak R, Florek W and Wałcerz R 1999 *J. Magn. Magn. Mater.* **203** 271
- [20] Kamieniarz G, Matysiak R, Caramico D'Auria A, Esposito F and Esposito U 1999 *J. Magn. Magn. Mater.* **196+197** 915
- [21] Atkinson I M, Benelli C, Murrie M, Parsons S and Winpenny R E P 1999 *J. Chem. Soc., Chem. Commun.* 285
- [22] Marvilliers A, Yu Pei, Boquera J C, Vostrikova K E, Paulsen C, Rivière E, Audière J P and Mallah T 1999 *J. Chem. Soc., Chem. Commun.* 1951